Holistic and Partial Face Recognition in the MWIR Band using Manual and Automatic Detection of Face-based Features

Nnamdi Osia and Thirimachos Bourlai
West Virginia University
PO Box 6201, Morgantown, West Virginia 26506
E-mail: nnamdi.osia@gmail.com, ThBourlai@mail.wvu.edu
Web: http://csee.wvu.edu/~tbourlai/

***Abstract*—Most of the benchmark face recognition (FR) approaches are designed to depend upon the usage of holistic or texture-based features of the human face. Here we present a new approach to the problem of middle-wave infrared (MWIR) facial recognition that realizes the full potential of the MWIR band. It consists, first, of a fully automated standardization of MWIR images prior to feature extraction through: skin segmentation, eye detection, inter-ocular and geometric normalization of our entire face dataset. Then, a statistically-based physiological feature extraction algorithm is used that is tailored to MWIR phenomenology: infrared-based features are extracted that consist of wrinkles, veins, edges, and perimeters of facial characteristics using anisotropic diffusion and top hat segmentation. At the next step, fiducial points are detected either manually, or automatically using different detectors such as a fingerprint-based minutiae detector, the Scale-Invariant Feature Transform (SIFT) detector, and the Speeded Up Robust Feature (SURF) detector. Finally, face matching is performed, utilizing fiducial points originally detected: end points and branch points on the face are filtered using the maximum pixel distance allowed between two matching points. Matching experiments are performed by using either the whole or sub-regions of the human face. Facial matching results on holistic faces emphasize the importance of data pre-processing as we achieve a rank-1 accuracy of at least 95%, independent of the fiducial point extraction method employed.**

I. Introduction

Face recognition (FR) has been a rapidly growing research area due to an increasing demand for biometric-based security applications. Varying factors such as cosmetics, illumination, and face disguise can hinder FR performance. One of the biggest challenges is the ability to recognize a person in both day and night time environments. In order to mitigate such a challenge, FR operation in the infrared (IR) spectrum (active and passive) has become increasingly important.

The active IR spectrum consists of the Near IR band ($0.7 - 0.9\ \mu\text{m}$) and the Short-Wave IR band ($0.9 - 2.5\ \mu\text{m}$). During data acquisition in the active IR band, the subjects face is usually illuminated using an external light source that can be detectable (NIR) or not (SWIR). The passive IR spectrum consists of the Mid-Wave IR (MWIR) band ($3 - 5\ \mu\text{m}$), and Long-Wave IR (LWIR) band ($7 - 14\ \mu\text{m}$). When data is acquired in the passive IR band, the camera sensor detects IR radiation in the form of heat that is emitted from the subjects face. Passive IR sensors provide a significant capability of acquiring human biometrics under obscure environments in a covert manner. Such a capability in combination with the usage of other IR sensors (SWIR) can result in improving the performance of FR systems in the dark.

Although the appearance of MWIR and LWIR face images is similar, both spectral bands capture different characteristics of the human face. MWIR has both reflective and emissive properties and works well for long distance operations. MWIR face images are normally not affected by external illumination. Also, unique physiological features for each individual, such as subcutaneous information (veins), edges of facial features, and wrinkles, are detectable in the MWIR band, which are useful for recognition. Finally, MWIR imaging is unobtrusive, and therefore FR in this band is more useful for both military and law enforcement applications.

Previous work in IR-based FR, such as Trujillo's et al. [17], proposed an unsupervised local and global feature extraction paradigm. Chen et al. [8] combined visible and IR images and compared them using Principle Component Analysis. Neither Trujillo or Chen's work focused in the MWIR band. Recently, Buddharaju et al. [6] used a MWIR-based face matcher that resulted in a rank-1 recognition rate of 84% for holistic frontal face images.

A. Goals and Contributions

In this paper we investigate a new, fully automated MWIR FR approach, applied on full-frontal face images acquired using a high-end MWIR sensor. The sensor is capable of delivering high definition images. In the pre-processing step, after automatic background subtraction, faces and eyes are automatically detected [3] and the faces are then geometrically normalized. Standard approaches are used during the pre-processing step to assist in error minimization. By the positioning of the eye centers at (x, y) locations at a standard spatial resolution, the inter-ocular distance is fixed. Prior to the feature extraction stage, all parameters for image diffusion and face segmentation are optimized. Unlike the method in [6], we determined that no dilation, skeletonization, or bridging was

978-1-4673-2709-1/12/$31.00 ©2012 IEEE

necessary. In our feature extraction step, fiducial points are detected either *manually* or *automatically*.

In the *automatic* mode, canonical (normalized) faces are used and minutia points are extracted from physiologically-based (when using subcutaneous facial characteristics) and geometrically based face features (e.g. eye edges and eyelashes), which are considered unique for each individual. In the *manual* mode, human experts have been used to annotate minutiae points that are visually perceived as important for recognition. Finally, in the matching and decision making step, an input image (probe) is matched with a stored template (gallery), after the application of our feature extraction scheme on each image. As a result, a matching score is obtained from our minutiae-based feature extraction method. If the score is less than a pre-defined threshold, the input image is considered to have successfully matched with the template. In addition, the matching algorithm is also optimized for fiducial points rather than minutiae points, and does not consider orientation. An overview of the methodology proposed in this work is illustrated in Fig.1.

The efficiency of our proposed algorithm is tested using both holistic faces as well as sub-facial regions. Aside from our proposed method, other automated methods used for feature extraction were SIFT and SURF. The FR results were automatically obtained by applying the aforementioned methods on both automatically as well as manually extracted features (spatial points) from MWIR faces images. Experiments were performed on a dataset of 50 subjects, which achieved rank-1 accuracy of at least 95% when using auto-extracted features. The manual feature extraction method as well as the proposed automatic feature extraction method are both comparable, achieving a rank-1 accuracy of 100%, for holistic faces. SIFT and SURF features resulted in a rank-1 identification rate of no more than 97%.

B. Paper Organization

The rest of this paper is organized as follows. Sections 2, 3, 4, and 5 describe the fully automated pre-processing approach used, MWIR based feature extraction, the fiducial points detection methods, and the matching approach we applied respectively. Conclusions and future work are described in Section 6.

II. Pre-Processing

A. Skin Segmentation

The first step of the pre-processing stage is segmenting the face from the subjects body, clothing and background noise to eliminate any artificial features. A blob detection algorithm is used to detect the bright portions of the face (skin) using a pre-determined threshold value. The threshold value for the blobs is the numerically larger pixel of the two intensity values that produce the greatest intensity difference. Using this threshold, a binary image is created, where pixel intensities above the threshold are assigned a value of one and pixel intensities below the threshold receive a value of zero. All blobs, which represent human skin, are analyzed and the largest one is selected. The human face is the largest uncovered area of skin in our images due to clothing, so the largest blob represents the MWIR face and neck. Background pixels (holes) inside the blob are then removed so that the mask is solid. The face blob is then used as a mask against the original MWIR image, setting the background and clothing black.

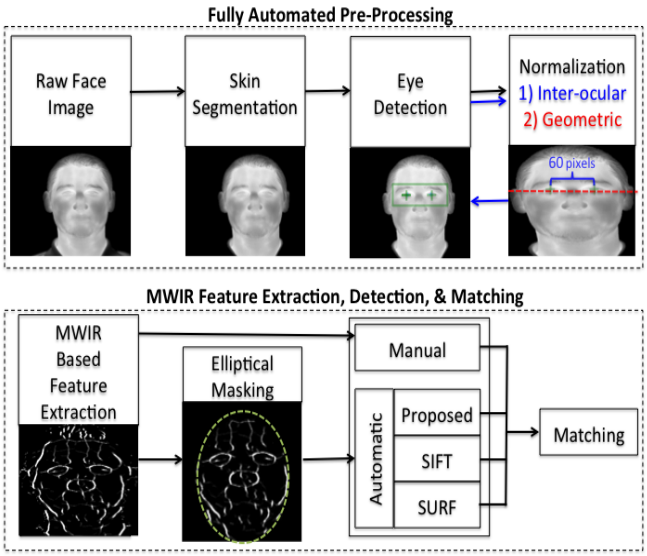

Fig. 1. **Overview of the methodology used to perform fully automated pre-processing, MWIR based feature extraction, fiducial annotation, and matching.**

B. Eye Detection

The problem of eye detection on MWIR images was studied by *Jafri and Bourlai* in [3]. This is the approach we selected to apply on our MWIR face images. First, the face is detected, which is trivial due to the previous skin segmentation method. Next, integral projections are used to find the general locations of the eyes and eyebrows on the face. Then, synthetic MWIR eye templates are created from the left and right eye of a number of subjects' face images. The generated templates are passed either (a) through each face side of an input face image, or, (b) when integral projections are employed, through the reduced search space that was determined by the location of the detected left and right eyebrows. The similarity score between the average eye template and a searched region is finally calculated using the Pearson Product Moment correlation coefficient. The highest correlation per search determines the location of each eye center. The coordinates of the eye centers obtained by this method are used for both the inter-ocular and geometric normalization of all of our MWIR face images.

C. Normalization

1) Inter-ocular Normalization: It standardizes all face images so head sizes are relatively similar. Once the eyes are detected on the MWIR images, they are used to normalize all images so that the inter-ocular distance is fixed to 60

pixels. This is accomplished by resizing the image acquired after skin segmentation using a ratio computed from the desired inter-ocular distance (60 px) and the actual inter-ocular distance, i.e. the one computed when using the image after skin segmentation.

2) Geometric Normalization: A geometric normalization scheme is applied to images acquired after inter-ocular normalization. The normalization scheme compensates for slight perturbations in the frontal pose, and consists of eye detection and affine transformation. Automated eye detection is performed once more using the same template matching algorithm described in *Step B* of our pre-processing approach described above (where the coordinates of the eye were automatically obtained). After the eye centers are found, the canonical faces are automatically constructed by applying an affine transformation. Finally, all faces are canonicalized to the same dimension of 320×256.

III. MWIR Based Feature Segmentation

The MWIR-based features extracted include: (a) veins, (b) edges, (c) wrinkles, and (d) face perimeter outlines (see Fig. 2).

A. Anisotropic Diffusion & Top Hat Segmentation

After pre-processing, the MWIR face images are further processed to remove background noise added during video acquisition and enhance edges by using the Perona-Malik anisotropic diffusion [15]. This is important because noise is reduced without the removal of significant MWIR image content, such as edges and lines. The mathematical representation for this process is described as follows:

$$\frac{\partial I(\bar{x},t)}{\partial} = \nabla(c(\bar{x},t)\nabla I(\bar{x},t)) \tag{1}$$

where, $I(\bar{x},t)$ is the MWIR image, $\bar{x}$ refers to the spatial dimensions, and t refers to time. $c(\bar{x},t)$, is referred to as the diffusion function, and describes the natural occurrence of heat diffusion in MWIR images. Generally, heat diffusion produces weak sigmoid edges during heat conduction, which in turn creates smooth temperature gradients at the intersecting boundary of multiple objects with dissimilar temperatures in contact. After the noise is reduced, the MWIR features (wrinkles, veins, edges, and perimeters) are segmented through the use of image morphology. In order to segment these MWIR features, which are brighter in temperature than surrounding parts of the MWIR face, a morphological top-hat filtering is employed.

$$I_{open} = (I \bigominus S) \bigoplus S, \tag{2}$$

$$I_{top} = I - I_{open} \tag{3}$$

I, I_{open}, and I_{top} are the original, opened, and white top hat segmented images, respectively. S is the structuring element, and $\bigominus$ and $\bigoplus$ are the morphological operations for erosion and dilation respectively. Parameters for Perona-Malik anisotropic diffusion process along with top hat segmentation, were empirically optimized to ensure the resultant MWIR image (see Fig. 2(ii)) does not contain noise, i.e. outlier edges that do not represent clear face-based physiological and geometrical features.

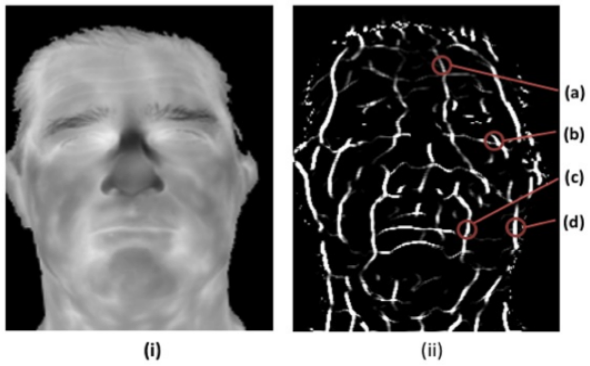

Fig. 2. **(i) Geometrically normalized face (before elliptical masking); (ii) Diffused and top hat segmented face (before elliptical masking): (a) veins, (b) edge, (c) wrinkle and (d) part of the face perimeter.**

B. Elliptical Masking

The final step before automatic detection of fiducial points is the application of an elliptical mask centered on the face image. It is imperative that the elliptical mask is applied after the feature extraction stage to ensure that spurious, artificial feature points are not created by the mask's presence during top hat segmentation. Having both skin segmentation and elliptical masking may seem a bit repetitive, but, in practice, image masking ensures no clothing is present during feature detection. When the face is segmented by the elliptical mask, the part of the original image that is masked is set to a black background. Note also that the dimensions of the ellipse used for all images was fixed.

IV. Experiments

A. Datasets

The camera used in this work is a high definition MWIR camera produced by FLIR Systems. It is capable of acquiring thermal-based imprints of human skin and analyzing the thermal distributions and temporal variations, corresponding to emission of $3-5\ \mu\mathrm{m}$ wavelength. The camera is capable of generating high definition thermal images and operating in diverse testing environments. It features a high resolution 1024×1024, and Indium Antimonide (InSb) Focal Plane Array (FPA), achieving mega-pixel image resolution in a single thermal image. The spectral range of the camera is $3-5\ \mu\mathrm{m}$, and it has a 14 bit dynamic range and a Noise Equivalent Temperature Difference (NEDT) of less than 25mK. The camera was outfitted with a 50 mm MWIR lens, also provided by FLIR Systems.

In total, 50 subjects (33 male + 17 female) participated in this experiment, and the database has 15 full frontal face MWIR images of each subject resulting in a total of 750

MWIR images. Only 4 samples out of 15 samples were used in total. The first two samples were the gallery images, while the other two samples were used as probe images, i.e. a total of 200 images (out of the 750 possible MWIR images) used in the extraction of MWIR features. As discussed before, a fully automated standardization of MWIR images is performed for all sets. In addition, different methods for automatic feature detection and manual feature detection are used on our MWIR subset.

B. Fiducial Points

Fiduciary points are used as points of measure in many face recognition applications and play an important role in our matching algorithm. The use of fiducial points is appropriate due to the permanent and unique nature of the extracted MWIR based features related to face-based subcutaneous information. Note also that although only face images with neutral expressions and poses were used in our experiments, fiducial points can be extracted and used for matching regardless of facial pose or expression.

In this work, after our MWIR based feature extraction, fiducial points are detected either manually, or automatically. In the latter case three different methods have been evaluated. All approaches are described below. The fiducial points detected by utilizing each approach in the case of a specific subject are illustrated in Fig. 3.

1) Manually Extracted Features: In order to achieve manual detection, a graphical user interface was created in MATLAB. All images (after MWIR-based feature extraction) are loaded randomly to avoid bias in manual feature detection between samples. Approximately one hundred minutia points were selected on each MWIR face image, and the average time required for the expert to complete manual annotation was about two to three minutes per image. About half of the selected points were detected on the upper half of the face, and the remaining half were selected on the lower half of the face. Priority was given to points around eyes, nose, mouth, cheeks, and forehead. Note that no elliptical masking was performed on the MWIR images used in manual extraction of fiducial points (see Fig. 1).

2) Automatically Extracted Features: Three different detectors are used such as a fingerprint-based minutiae detector, the SIFT detector, and the SURF detector.

– *Fingerprint-based Minutiae Detector:* It was proposed at [21] and in this work it was applied to the face images of our MWIR dataset. In terms of normalization, the mean pixel intensity of the features extracted from each MWIR image is set as the threshold for binarization. While traversing through the image, if the current pixel intensity is smaller than the threshold, it is set to zero; if otherwise, it is set to one. Note that pixel normalization was the only pre-processing performed on the images. During the traversal process, if the 3×3 neighborhood around a center pixel of value 1 had exactly three one-valued pixels, it was labeled a branch point. If the center pixel is 1 and the 3×3 neighborhood around the pixel contains only 1 one-value neighbor, then it is labeled an end-point. Depending on the normalization technique, large clusters of minutiae (both branch points and end points) may be found. A very small number of spurious minutiae points, which maybe a result of our automated pre-processing pipeline, are

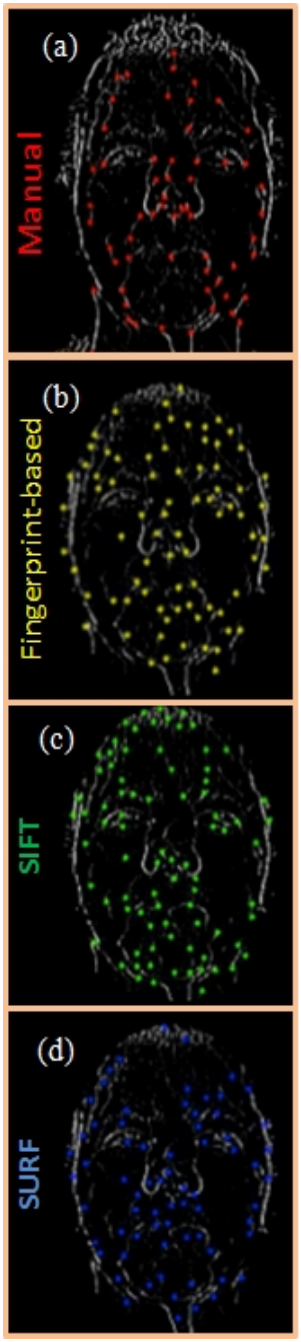

Fig. 3. **MWIR face with: (a) Manually detected points [red], (b) Fingerprint-Based Minutiae detected points [yellow], (c) Scale-Invariant Feature Transform detected points [green], and (d) Speeded Up Robust Feature detected points [blue], considered critical for recognition.**

removed prior to matching. Both sets of points are also filtered independently, using the maximum pixel distance allowed between two matching points.

– *Scale-Invariant Feature Transform (SIFT):* The SIFT algorithm used in this work is able to identify both feature detectors and feature descriptors. The detector extracts a number of frames from an image in a manner that is consistent with certain variations that may affect image quality such as external illumination. The descriptor marks the regions in order to identify their appearance compactly and robustly. The features detected are invariant to scaling or rotation, translation, and partially invariant to illumination changes. The SIFT feature detector was required in our work because we are only interested in x-coordinate and y-coordinate points (distinct feature key points). Such points are defined as resultant maxima and minima of Difference of Gaussians (DoG) applied to smoothed and re-sampled images. The Gaussian kernel is used because its derivatives are considered as the smoothing kernels for scale space analysis. By choosing to select key maxima and minima locations, from the DoG function applied in the scale space, the features detected become invariant to rotation. While the 2D Gaussian function is distinguishable, its convolution with the input image can be computed by applying two iterations of the 1D Gaussian function in both horizontal and vertical directions:

$$g(x) = \frac{1}{\sqrt{2\pi\sigma}} e^{-x^2/2\sigma^2} \tag{4}$$

In implementation, our SIFT detector is controlled primarily by two parameters, the peak threshold and the non-edge threshold. The peak threshold filters peaks of the scale-space that are too little in absolute value. As the peak threshold increases, fewer features are obtained. The edge threshold removes peaks of the DoG scale-space whose curvature is miniscule. As the edge threshold increases, more features are obtained. After applying this detector, for each key feature location, the x-axis and y-axis coordinates are extracted.

– *Speeded Up Robust Feature (SURF):* The SURF method is very similar to SIFT. However, SURF is only a scale and rotation-invariant interest point detector and descriptor, offering a compromise between feature complexity and robustness for commonly occurring deformations. An added benefit of avoiding the excess of rotation invariance in such cases is increased speed. The use of integral images allows for fast implementation of box type convolution filters. By relying on integral images for image convolution, SURF achieves distinctiveness and robustness. SURF aims to find salient regions in near constant time through its use of integral images and box filters. The SURF detector is based on the Hessian matrix due to its good performance in computation time and accuracy. Given a point x = (x, y) in an image I, the Hessian matrix $H(\mathrm{x}, \sigma)$ in x at scale σ is defined as follows:

$$H(\mathrm{x}, \sigma) = \begin{bmatrix} L_{xx}(\mathrm{x}, \sigma) & L_{xy}(\mathrm{x}, \sigma) \\ L_{xy}(\mathrm{x}, \sigma) & L_{yy}(\mathrm{x}, \sigma) \end{bmatrix} \tag{5}$$

where $L_{xx}(\mathrm{x}, \sigma)$ is the convolution of the Gaussian second order derivative $\frac{\partial^2}{\partial x^2} g(\sigma)$ with the image I in point x, and similarly for $L_{xy}(\mathrm{x}, \sigma)$ and $L_{yy}(\mathrm{x}, \sigma)$. The box filter used in the SURF algorithm is a further approximation of the Laplacian of Gaussian (LoG) methodology originally used by Lowe in the SIFT algorithm [11]. When features are detected using the SURF algorithm, there is no need to iteratively apply the same filter to the output of a previously filtered level images. By taking the discrete nature of integral images and specific structure of our filters into consideration, the subsequent levels are acquired by filtering the image with gradually larger masks. After obtaining x-coordinate and y-coordinate, we move on to applying our matching algorithm using the detected points generated by SURF.

V. Matching

Instead of using a local or global matching scheme, the potential match space is maximized through the use of a brute force matching approach. An alignment-based matching algorithm with the ability of finding the correspondences between a stored set of gallery points and input set of probe points is used [9]. The set input points are first aligned with the gallery and then, match score is computed, based on max matched points. We let $G = ((x_i^G, y_i^G)^T, ..., ((x_i^G, y_i^G)^T))$ and $P = ((x_j^P, y_j^P)^T, ..., ((x_j^P, y_i^P)^T))$ denote the G Cartesian points in the gallery set and the P Cartesian points in the input probe set, with lengths M and N respectively. The algorithm is exhaustive and considers all possible pairings of x-axis and y-axis points in each set. The distance between each possible point in the gallery set and point in the probe set is computed and sorted in increasing order. Then, the number of matches below a threshold (the maximum allowable pixel distance between two matching points) is counted. The highest counted number of correspondences; C_{best}, for each set of points is stored and used to compute the match score, M_S (see Equation 6 below).

$$M_S = \frac{(C_{best})^2}{sum\{M, N\}} \tag{6}$$

A. Matching using Holistic MWIR Face Images

The performance of our proposed approach was evaluated on holistic face image and compared against other commercial (Identity Tools G8) and academic (CSU Face Identication Evaluation System) FR software. The results are summarized in Fig. 4. Experimental results illustrate that our proposed method outperforms the other techniques in terms of rank-1 identification rates. Another advantage is that our approach is based on direct matching among gallery and probe images,

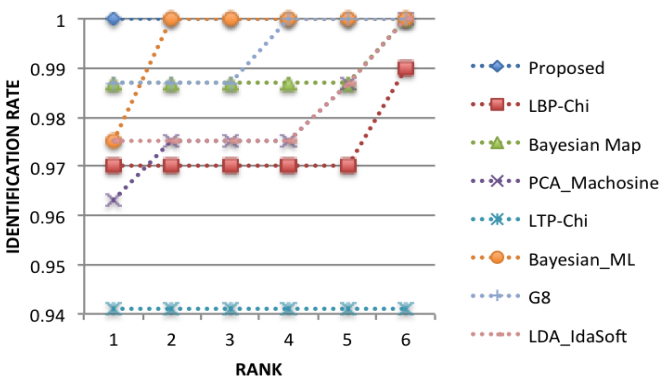

Fig. 4. **Identification rates (Rank-1 to Rank-6) when using holistic MWIR face images.**

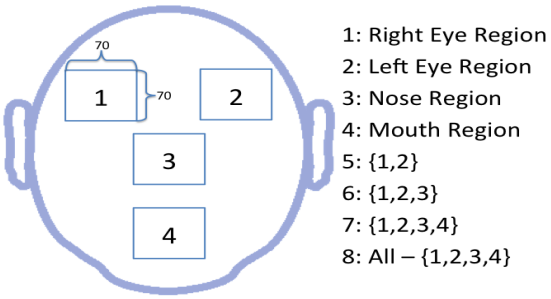

Fig. 5. **Face template for regions of face matched using 70x70 windows.**

eliminating the need of having to design and use a training set.

B. Matching using Sub-Facial MWIR Face Images

In this set of experiments, the automatically detected points extracted from holistic face images are partitioned depending on specific face regions, i.e. left eye, right eye, nose, chin, both eye regions, both eye and nose regions, both eye and nose regions along with the chin regions, and finally all disjoint points that are not in any aforementioned regions, but still part of the set (see Fig. 5 above). Each sub-region (e.g. left or right eye, nose and chin) is extracted using a 70×70 window around user-specific selected points centered on the left eye, right eye, nose, and chin respectively (see Fig. 6). Our automatic feature extraction method is evaluated against manual point detection, and automatic point detection methods (SIFT and SURF), for all parts of the face. Note that all manual detected, SURF detected, and SIFT detected feature points were constrained to no more than 100 feature points. On the other hand, our automatic method was constrained depending on the maximum pixel distance allowed between two matching points. The results are summarized in Table 1.

TABLE I
IDENTIFICATION RESULTS AT RANK-1 (%) FOR HOLISTIC AND INDEPENDENT FACIAL FEATURES OF MWIR IMAGES

Region(s) Selected	Manual	Proposed	SIFT	SURF
Whole Face	100	100	97	95
Left Eye	75	52	43	22
Right Eye	75	62	43	22
Nose	82	73	43	39
Chin	82	66	36	14
Eyes	95	82	72	52
Eyes and Nose	97	92	86	69
Eyes, Nose, Mouth	99	100	93	72
Disjoint	97	99	94	84

VI. DISCUSSION & CONCLUSIONS

In this paper, we presented a new approach to the problem of middle-wave infrared facial recognition that realizes the full potential of the MWIR band. We also performed an evaluation study on the efficiency of our approach compared to different feature extraction methods and FR matching algorithms based on identification performance. For that purpose, our MWIR face database was used. The experiments carried out were not only performed using holistic faces but face sub-regions and their combinations as well, such as eye, nose, and chin regions.

When using fiducial points that were manually annotated, we achieved the best overall identification performance (in terms of rank-1 rates) for the whole face as well as in the majority of the sub-facial regions, and their combinations. This is considered a very interesting result. However, we need to point out that the identification rates when using manual annotated face images were achieved on the original MWIR feature extracted image, i.e. before the elliptical masking is applied. Thus, the availability of more facial information may be the reason of why the manual results were higher than the automatically obtained ones.

Another advantage to our proposed approach is that it is fully automated and does not require a design and the usage of a training set. This saves a lot of computational time and effort. Another observation is that even though we only dealt with frontal face images, the design of our pre-processing step turned to be very important in achieving high recognition rates. Furthermore, although users could be identified using parts of the face instead of the whole face, face sub-regions should be used in conjunction with other biometric approaches to boost performance. We also understand that due to the scarcity of MWIR face images, there does not exist enough face data to make any statistically valid claims regarding using any FR approach for matching.

A very interesting result from our study was in the case where our proposed methodology was applied to the disjointed face sub-region (i.e. the region of the face excluding the eyes, nose, and chin regions). In this case we achieved a 99% rank-1 identification rate, suggesting that the features extracted around the cheek and forehead regions are unique per individual. This needs further investigation, and if such an

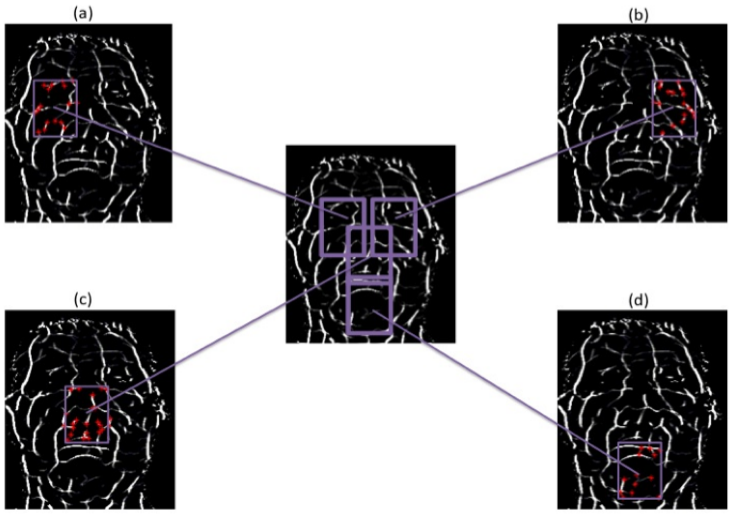

Fig. 6. **Sample subject image of independent face region and detected features: (a) Left Eye, (b) Right Eye, (c) Mouth and (d) Chin regions.**

observation holds in large datasets, it can assist current FR systems in cases of facial occlusion or disguise.

Following that, the application of our proposed methodology to datasets consisting of subjects with facial occlusion or disguise intending to counterfeit a biometric system would provide further insights in this research field. Also, to further validate the efficiency of our proposed FR approach, other datasets such as that of the University of Notre Dame [14] should also be considered. Future work should also include statistical analysis of why manually extracted features result in higher recognition rates than automatically extracted ones.

ACKNOWLEDGMENT

This work is sponsored in part through a grant from the Office of Naval Research (ONR), contract N00014-09-C-0495, and support from the NSF Center for Identification Technology Research (CITeR), award number IIP-0641331. We would like to acknowledge Dr. A. Ross and Dr. L. Hornak for their valuable input during the initial phase of this work as well as all WVU faculty and students that contributed in various parts of this research effort.

REFERENCES

[1] H. Bay, A. Ess, T. Tuytelaars, and L. Gool, "SURF: Speeded Up Robust Features," *Computer Vision and Image Understanding (CVIU)*, vol. 110, no. 3, pp. 346-359, 2008.

[2] D. Bolme, J. Beveridge, M. Teixeira, and B. Draper, The CSU face identification evaluation system: Its purpose, features and structure, *Proc. International Conference on Vision Systems*, 304-311, 2003.

[3] T. Bourlai, Z. Jafri, "Eye detection in the Middle-Wave Infrared spectrum: Towards recognition in the dark", *IEEE Intl. Workshop on Information Forensics and Security (WIFS)*, 2011.

[4] T. Bourlai, A. Ross, C. Chen, and L. Hornak, "A Study on using Middle-Wave Infrared Images for Face Recognition," *SPIE, Biometric Technology for Human Identification IX*, Baltimore, U.S.A., Apr. 2012.

[5] P. Buddharaju, I. Pavlidis, and P. Tsiamyrtzis, "Pose-Invariant Physiological Face Recognition in the Thermal Infrared Spectrum," *Proc. 2006 IEEE Conf. Computer Vision and Pattern Recognition*, pp. 53-60, June, 2006.

[6] P. Buddharaju, I. Pavlidis, P. Tsiamyrtzis, and M. Bazakos, "Physiology-Based Face Recognition in the Thermal Infrared Spectrum," *IEEE Transactions on Pattern Analysis and Machine Intelligence*, vol. 29, no.4, pp. 613-626, 2007.

[7] P. Buddharaju, I. Pavlidis, C. Manohar, "Face Recognition Beyond the Visible Spectrum", *Advances in Biometrics: Sensors, Algorithms and Systems*, pp. 157-180, Springer London, Nov. 2007.

[8] X. Chen, P. Flynn, and K. Bowyer, "PCA-Based Face Recognition in Infrared Imagery: Baseline and Comparative Studies", *In Proceedings of the IEEE International Workshop on Analysis and Modeling of Faces and Gestures (AMFG)*, 2003.

[9] A. K. Jain and L.Hong, "On-line fingerprint verification", *IEEE Transactions on Pattern Analysis and Machine Intelligence*, vol. 19, no. 4, pp. 302-314, 1997.

[10] X. Jiang and W. Yau, "Fingerprint Minutiae Matching Based on the Local and Global Structures," *Proc. 15th Intl Conf. Pattern Recognition*, vol. 2, pp. 1038-1041, Sept. 2000.

[11] D. Lowe, "Object recognition from local scale-invariant features," *Proceedings of the International Conference on Computer Vision*, pp. 1150-1157, 1999.

[12] D. Lowe, "Distinctive image features from scale-invariant keypoints," *Int. J. Computer Vision 60*, 91-110, Nov., 2004.

[13] J. Miller, "Principles Of Infrared Technology: A Practical Guide to the State of the Art", Springer, 1994.

[14] Biometrics Database Distribution, The Computer Vision Laboratory, Univ. of Notre Dame, http://www.nd.edu/cvrl/, 2002.

[15] P. Perona and J. Malik, Scale space and edge detection using anisotropic diffusion, *In Proc. IEEE Workshop Comput. Vision*, Miami, FL, Nov. 1987, pp. 16-22.

[16] A. Oliveira and N.J. Leite, "Reconnection of Fingerprint Ridges Based on Morphological Operators and Multiscale Directional Information," *Proc. 17th Brazilian Symp. Computer Graphics and Image Processing*, pp. 122-129, Oct., 2004.

[17] L. Trujillo, G. Olague, R. Hammoud, and B. Hernandez, "Automatic Feature Localization in Thermal Images for Facial Expression Recognition," *Proceedings of the 2005 IEEE Computer Society Conference on Computer Vision and Pattern Recognition (CVPR)* Vol. 3, 2005.

[18] A. Vedaldi, B. Fulkerson, "Vlfeat: an open and portable library of computer vision algorithms," ACM Multimedia 2010: 1469-1472.

[19] J. Wang, E. Sung, and R. Venkateswarlu, Registration of Infrared and Visible-Spectrum Imagery for Face Recognition, *Proc. Sixth IEEE Intl Conf. Automatic Face and Gesture Recognition*, pp. 638-644, May, 2004.

[20] S. Yang and I.M. Verbauwhede, "A Secure Fingerprint Matching Technique," *Proc. 2003 ACM SIGMM Workshop Biometrics Methods and Applications*, pp. 89-94, 2003.

[21] W. Zhili, "Fingerprint Recognition," Ph.D. Thesis, Honk Kong Baptist, University, 2002.